

Behaviour of α - Al_2O_3 insulator surfaces under electron irradiation

C. JARDIN, P. DURUPT, D. ROBERT, P. MICHEL
*Laboratoire de Minéralogie-Cristallographie (URA CNRS 805),
 Université Claude Bernard Lyon I, 43 Boulevard du 11 Novembre 1918,
 69622 Villeurbanne Cedex, France*

C. LE GRESSUS
CEA-IRDI, CEN Saclay-91191 Gif-sur-Yvette, France

Cathodoluminescence (CL), Auger electron spectroscopy (AES) and direct crack measurements were performed on α - Al_2O_3 samples in order to relate chemical, electrical and mechanical effects induced by electron irradiation of the surface. Electrical discharges and visible luminescence were observed during the excitation of the samples with a 80 keV electron beam. Changes of the surface state and of the toughness K_{Ic} were subsequently detected.

The results suggest that charging of the sample is related to the presence of defects and corresponding trap levels in the energy gap. The concentration of defects (oxygen vacancies or associated F, F^+ centres) may be enhanced, especially in the vicinity of the surface, by the electrical discharges induced by the electron irradiation. This leads to an increase of mechanical stresses in the brittle material: a striking example was the fracture of a corundum single crystal in the electron microscope, which cannot be explained by the direct heating effect of the primary electron beam. On the contrary, an advantageous situation for the mechanical properties of the material may be achieved when the defects have a blocking effect on the crack propagation; a subsequent increase of the toughness K_{Ic} is then recorded.

1. Introduction

Charging of insulator samples is usually considered as an experimental difficulty in electron microscopy and electron spectroscopies, indeed, a shift of the kinetic energy, broadening of the lines and anomalous structures are often observed in Auger electron spectroscopy of insulators (Fig. 1). Distortion of the images and deflection of the beam due to surface charging are well known disturbances in electron microscopy (Fig. 2). The magnitude of the surface charge is dependent on the ability of the sample to drain off the current $I_P - I_R$ (I_P and I_R are, respectively, the primary and backscattered electron beam intensities), which is related to the nature of the material, its electrical surroundings and also to the excitation parameters [1–5].

It has been demonstrated experimentally by different authors [6–8] that charge-up problems on insulators are greatly reduced for clean, perfectly crystalline and stoichiometric surfaces. Furthermore, removal of the chemical beam effects often induces a decrease of the electrical ones [8]. These results denote the significant role played by defects such as impurities, vacancies and dislocations and their corresponding trap levels in the forbidden band, on the charge phenomena of insulator surfaces [9].

2. Mechanical breakdown of a strained corundum single-crystal

Combined chemical and electrical effects due to elec-

tron irradiation of insulator surfaces lead to a change in their mechanical properties. A striking example was the mechanical breakdown of a corundum α - Al_2O_3 single crystal under electron excitation. The sample, in the form of a plate $2 \times 10 \times 0.5 \text{ mm}^3$ in dimensions, was subjected to an initial elastic mechanical strain using a special holder; this sample was then introduced into a vacuum chamber (10^{-5} torr) and exposed to an 80 keV electron beam. The fracture of the specimen was observed after an irradiation time of about 3 s! Such damage cannot be explained by the direct heating effect due to the primary beam. A temperature rise of less than 100°C was deduced from the disc heating model of Vine and Einstein [10] using our experimental conditions

$$\Delta T = (0.099 I_p E_p) / (\pi^{0.5} K a) = 75^\circ\text{C}$$

where I_p is the primary current = 2×10^{-5} A; E_p the electron energy = 80 000 eV; a the beam radius = 0.02 cm and K the thermal conductivity of corundum = $0.06 \text{ cal cm}^{-1} \text{ }^\circ\text{C}^{-1} \text{ s}^{-1}$. Optical microscopy observation of the irradiated surface of the damaged sample reveals the presence of electrical discharge lines (Fig. 3). Combined chemical and electrical effects are thus certainly responsible for the observed phenomena, and two possible interpretations are proposed.

(i) The applied mechanical strain has generated localized defects in the crystal resulting in a significant

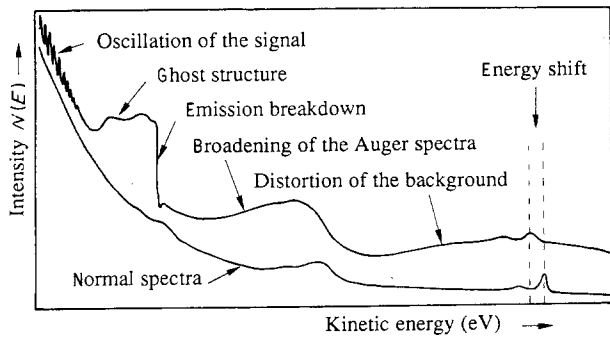


Figure 1 Schematic illustration of the $N(E)$ secondary electron emission of anomalous structures due to surface charging of an insulator.

trapping of electrons under the incident beam. This may induce the breakdown of the specimen under the influence of Coulomb repulsion forces.

(ii) Electrical discharges and related defects are generated by electron irradiation of the crystal. An additional mechanical strain induced by these defects superimposes on the initial one to reach the elastic limit of the brittle material. This later assumption is in better agreement with the observed change of the toughness K_{Ic} against the electron irradiation dose, which is discussed in the next section.

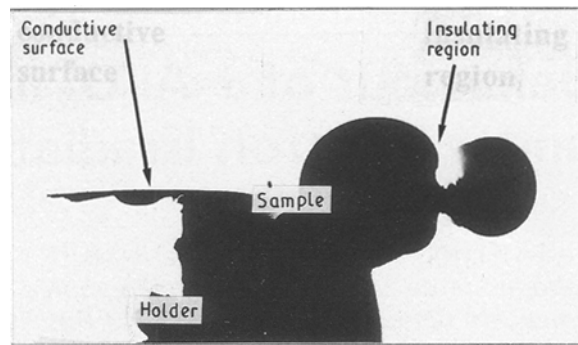


Figure 2 Behaviour of a polymer film (kapton polyimide) under a 80 keV grazing incident electron beam. The surface of the sample includes an area previously irradiated with 500 keV nitrogen N^+ ions. Electrostatic bubbles due to surface charging are observed on the insulating part of the material whereas the N^+ irradiated region is conductive.

3. Electrical discharges on $\alpha\text{-Al}_2\text{O}_3$ samples

Different $\alpha\text{-Al}_2\text{O}_3$ samples (corundum single-crystal, polycrystalline alumina) with mirror-polished surfaces were exposed to a defocused electron beam of 80 keV energy for a few hours in a 10^{-5} torr vacuum. Cathodoluminescence and electrical discharges on the sample occurred during electron irradiation. The

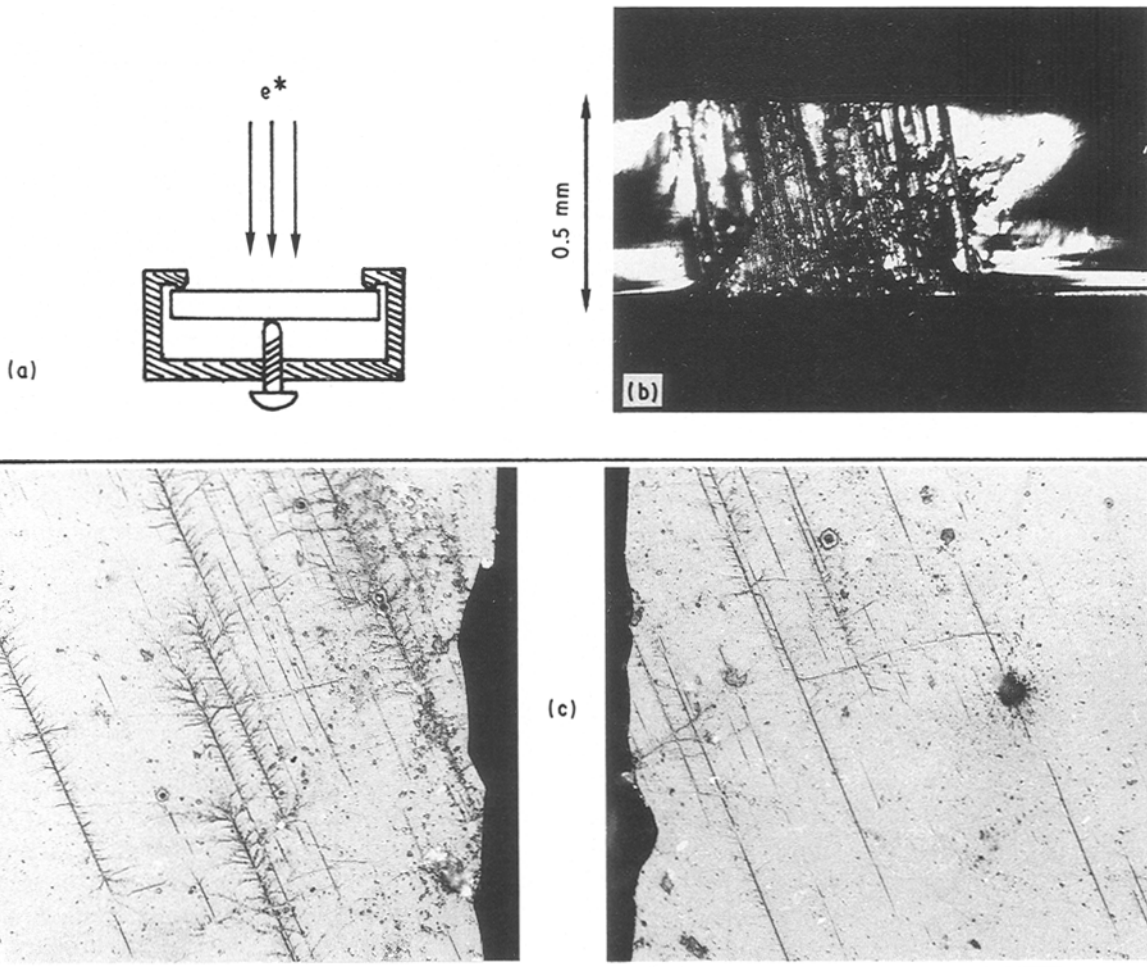


Figure 3 Mechanical breakdown of a corundum single-crystal $\alpha\text{-Al}_2\text{O}_3$ induced by electron irradiation. (a) Sample holder allowing the application of an initial elastic strain to the specimen. Optical microscopy photographs of; (b) the broken surface and; (c) the two parts of the crystal surface after the beam damage including electrical discharge marks.

frequency of the flashovers was found to increase with irradiation time.

Traces of the electrical discharges on the insulator surface, as observed by optical microscopy, are shown on Fig. 4. Geometrical lines are detected on corundum single crystals; they correspond to the residual polishing streaks, revealed by the electrical discharges which have gone along these preferential paths. For polycrystalline alumina, the tree-like figure of the flashovers may be explained by the lack of dominant preferential tracks, or by the presence of randomly distributed paths offered by the boundaries of the crystalline grains of 1 μm mean size which is comparable to the dimension of the residual defects after the polishing procedure. As shown on Fig. 4b, metallic

silver islands deposited on the single-crystal $\alpha\text{-Al}_2\text{O}_3$ are active centres for the electrical breakdown of the irradiated sample. These observations point out that surface flashovers preferably occur through the regions of maximum concentration of chemical and structural defects.

4. Change of the toughness K_{Ic}

The toughness K_{Ic} of the irradiated material was deduced from direct crack measurements of the mean size ($2a$) of the Vickers figure and the mean length ($2c$) of the cracks induced by the indentation, using the empirical relation proposed by Liang, Orange and

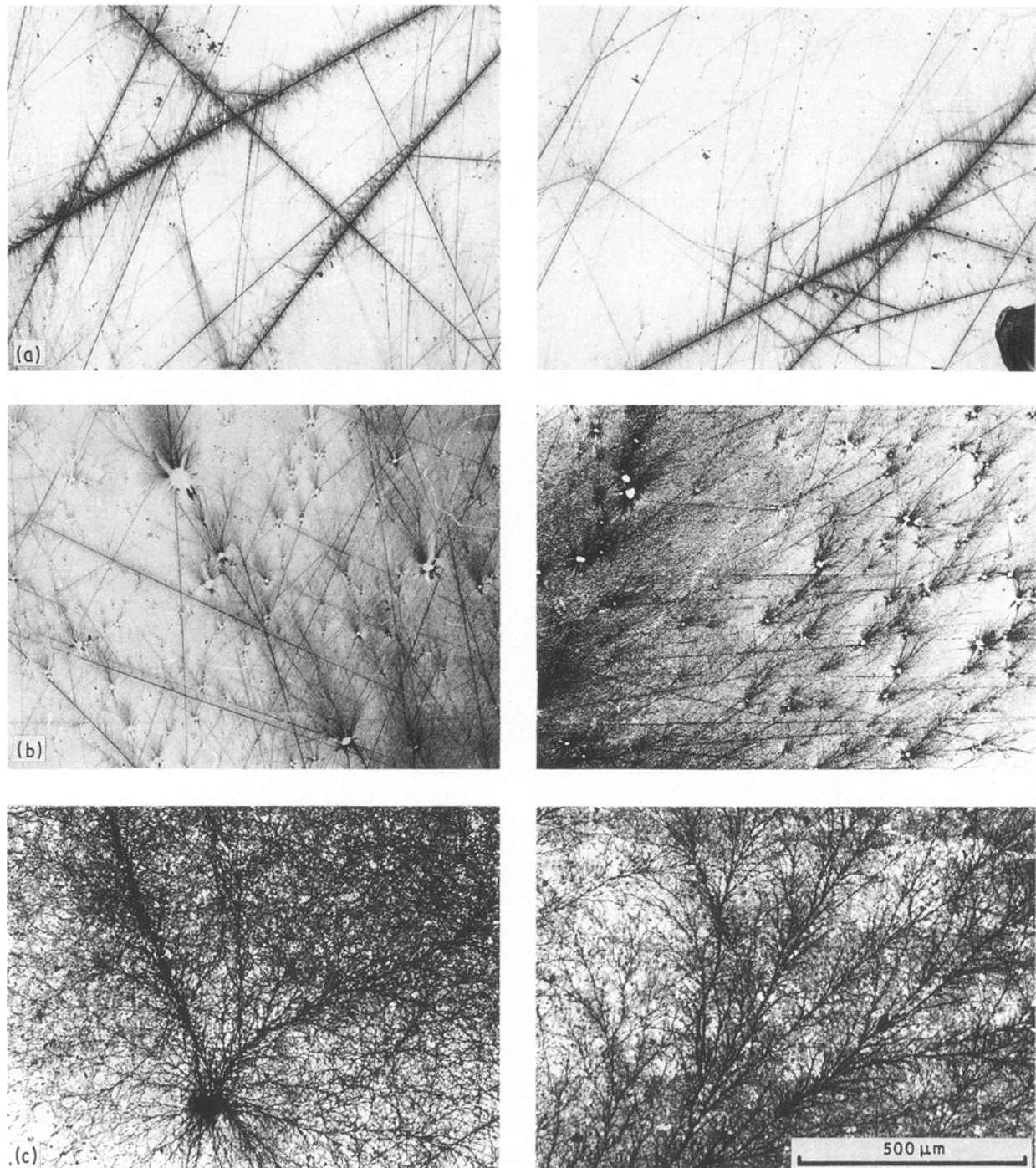


Figure 4 Optical microscopy images of $\alpha\text{-Al}_2\text{O}_3$ surfaces after electron irradiation (80 keV). Different electrical discharge figures are observed on (a) corundum single crystal; (b) corundum single crystal with deposited silver islands and; (c) polycrystalline alumina.

$$\frac{3 K_{Ic}}{H_v a^{1/2}} \cdot \left(\frac{H}{3E}\right)^{0.4} \alpha = \left(\frac{c}{a}\right)^{c/18a-1.51}$$

$$\alpha = 14\{1 - 8[(4\nu - 0.5)/(1 + \nu)]^4\}$$

where K_{Ic} is the toughness ($\text{MPa m}^{1/2}$); H_v the Vickers hardness (GPa); E the Young modulus (GPa) and ν the Poisson coefficient.

As shown in Fig. 5, the toughness K_{Ic} of the corundum crystal suffers a typical change with the exposure of the surface to the electron beam ($E_p = 80 \text{ keV}$; $J_p = 10^{-3} \text{ A cm}^{-2}$), whereas the Vickers hardness remains almost constant ($H_v = 22 \text{ GPa}$).

The decrease of K_{Ic} observed at medium electron dose is interpreted by considering the presence of beam induced defects (oxygen vacancies and related F , F^+ centres detected by cathodoluminescence [12]). This leads to a strained crystal and, as a result, to a more brittle material.

The content of defects and the electrical flashovers are enhanced by a prolonged irradiation; internal strains become too important for the crystalline structure to be maintained. Relaxation of the material occurs by a precipitation of point defects which deviates and restrains the crack propagation induced by the Vickers indentation. This situation corresponds now to an increase of the toughness K_{Ic} , and also agrees with the wavering paths of cracks observed on the irradiated surfaces.

5. Cathodoluminescence and AES results

Cathodoluminescence of the corundum crystals was performed at room temperature during electron

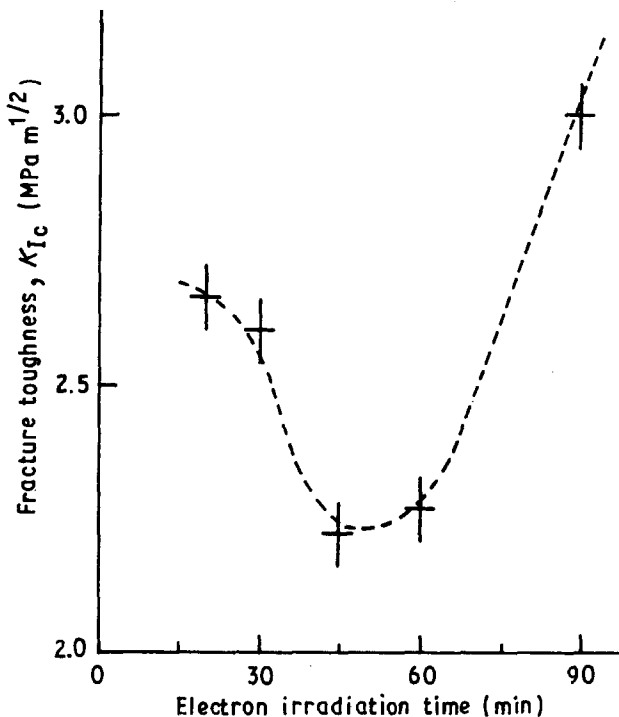


Figure 5 Change of the toughness K_{Ic} with the exposure time of a corundum crystal to the electron beam ($E_p = 80 \text{ keV}$; $J_p = 10^{-3} \text{ A cm}^{-2}$). Values of K_{Ic} were deduced from direct crack measurements, with a load $P = 1 \text{ N}$ for the Vickers indentation.

irradiation at 80 keV. A typical spectrum for the material, corrected for photomultiplier response and grating efficiency, is shown on Fig. 6; three main emissions at 1.7 eV (red emission), 3 eV (blue band) and 3.7 eV (near u.v. band) are observed.

(i) The red emission, with the characteristic 695 nm (1.8 eV) narrow band and the fine structures due to the crystalline environment, is attributed to chromium Cr^{3+} substitutional impurities. The concentration of this impurity is less than the AES detection level (about one atom per cent of the surface monolayer). This luminescence is similar to the CL red band of ruby ($\text{Al, Cr}_2\text{O}_3$). The 695 nm emission occurs as a result of the electronic transition ${}^2E \rightarrow {}^4A_2$ between the Cr^{3+} ion levels situated in the energy gap of the insulator without participation of the conduction and valence bands.

(ii) The blue and near u.v. bands are related to the beam induced defects because of their dependence on the experimental parameters. According to previous data [13–16] and our AES results, these defects are oxygen vacancies (F^{2+}) or associated F^+ and F centres (oxygen ion vacancies containing one and two electrons, respectively). The intensity of the near u.v. band is enhanced by an increase of the current density J_p of the incident electron beam and is also dependent on the crystal thickness. On the contrary, the relative intensity of the blue band – compared to the near u.v. emission – is stimulated at low current density (Fig. 7). This blue emission at 3 eV is attributed to intrinsic relaxation of the F centres, the concentration of which is enhanced by the following process: under the primary excitation, electrons injected in the conduction band are accelerated by the induced electrical field; these hot electrons can acquire sufficient kinetic energy to excite atoms and generate defects, leading also to the electrical breakdown of the material [17]. Such effects, as well as the near u.v. luminescence, are very efficient at higher J_p values. The near u.v. band at 3.7 eV would correspond to the F^+ centre emission usually detected at 3.8 eV in other experiments [13–16]. These F^+ centres are mainly produced by the transformation of F and F^{2+} centres in the presence of the electron beam.

The mechanisms involved in the 3 and 3.7 eV emission are schematically condensed as follows: (asterisk * denotes an excited state)

- (1) $F + \text{electron excitation} \rightarrow (F)^* \rightarrow F + h\nu (3 \text{ eV})$
(low J_p)
 - (2) $F + \text{electron excitation} \rightarrow (F^+)^* + e^-$
(high J_p)
- $(F^+)^* \rightarrow (F^+) + h\nu (3.7 \text{ eV})$
hot electron in the \rightarrow electrical discharge and
conduction band formation of new F^{2+}
defects and reaction 3
- (3) $(F^{2+}) + e^- \rightarrow (F^+)^* \rightarrow (F^+) + h\nu (3.7 \text{ eV})$

The interpretation of CL spectra based on oxygen vacancies or related F and F^+ centres is consistent with the next AES analysis: O-KLL oxygen Auger spectra of the crystal previously irradiated at 80 keV has a lower intensity than the standard sample (Fig. 8).

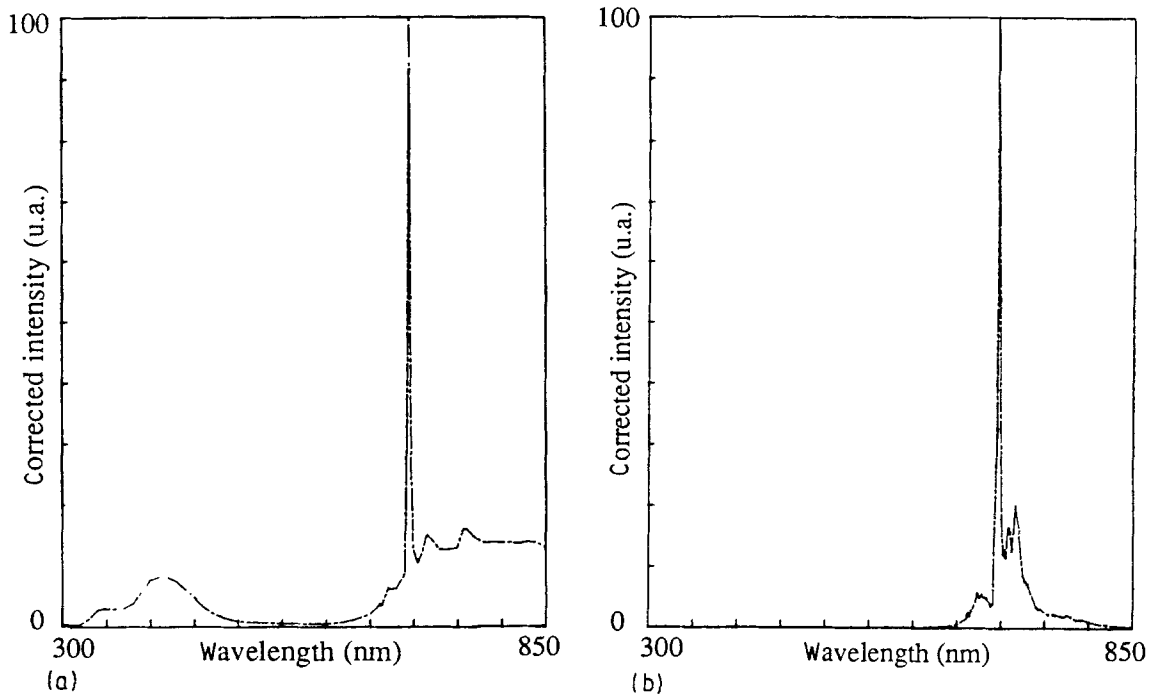


Figure 6 Typical cathodoluminescence spectra excited by a 80 keV electron beam from (a) corundum crystal $\alpha\text{-Al}_2\text{O}_3$; (b) red ruby crystal for comparison.

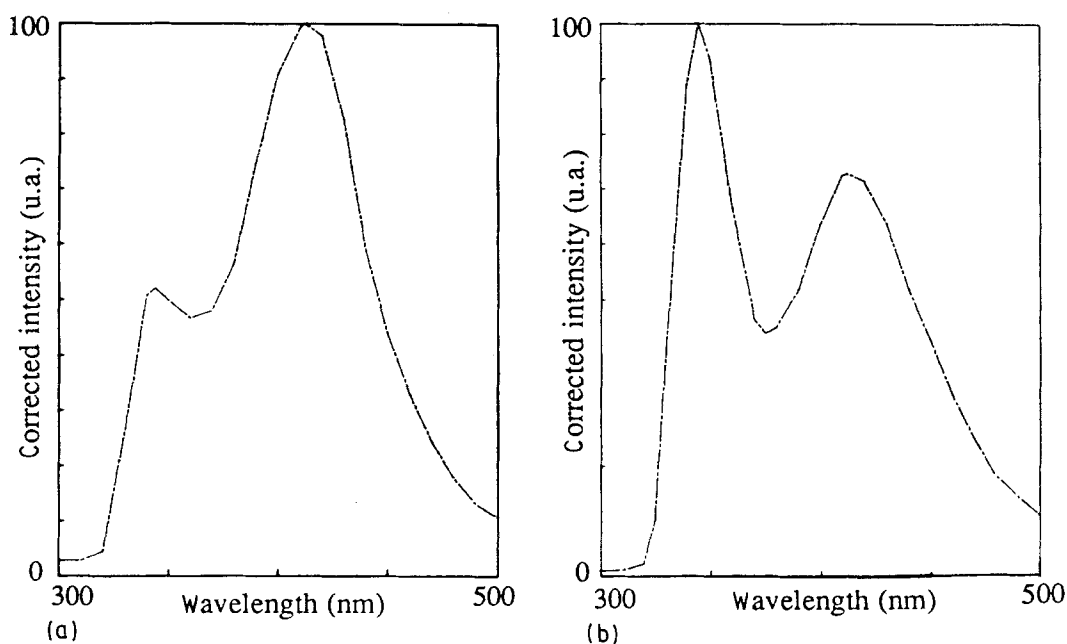


Figure 7 Change of the blue and near u.v. cathodoluminescence of a corundum crystal with the current density J_p of the incident electron beam. (a) Low J_p ($\leq 10^{-5} \text{ A cm}^{-2}$). (b) High J_p ($\geq 10^{-3} \text{ A cm}^{-2}$).

Furthermore, its surface appears chemically and electrically less homogenous; this is deduced from the energy shifts and intensity changes of the Auger spectra during the scanning of the sample with the primary Auger beam.

6. Conclusion

In this paper, we have attempted to demonstrate that chemical, electrical and mechanical effects induced by electron irradiation of an insulator surface are closely related. Macroscopic phenomena such as mechanical breakdown of a corundum crystal stimulated by the

electron beam, change of the toughness K_{Ic} and electrical discharges on the irradiated surface have been observed and interpreted. The significant role of defects, especially oxygen vacancies and related F , F^+ centres for the investigated $\alpha\text{-Al}_2\text{O}_3$ samples, and the cumulative effect between chemical and electrical damages have been pointed out.

Further investigations are in progress to determine the influence of the electron irradiation dose on the toughness of the material, to specify the surface effects (flashovers, surface defects, impurities) in the cathodoluminescence spectra and to compare the behaviour of different ceramic compounds.

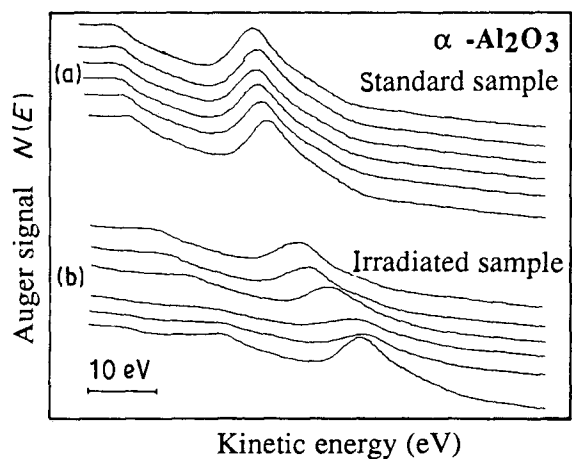


Figure 8 Change of the O-KLL Auger spectra with the scanning of the surface by the 2 keV primary Auger beam. (a) Standard corundum crystal; (b) after 80 keV electron irradiation.

Acknowledgements

The authors are grateful to M. Carre (UCB Lyon) for helping with cathodoluminescence experiments and to K. Liang, G. Orange and G. Fantozzi (INSA Lyon) for helping with direct crack measurements.

References

1. L. LEY, R. A. POLLAK, F. R. McFEELY, S. P. KOWALCZYK and D. A. SHIRLEY, *Phys. Rev.* **B9** (1974) 600.
2. M. W. ROBERTS and R. St. C. SMART, *Chem. Phys. Lett.* **69** (1980) 234.
3. J. CAZAUX, *J. Appl. Phys.* **55** (1986) 1418.
4. *Idem*, *J. Microsc. Spectrosc. Electron.* **11** (1986) 293.
5. M. BRUNNER and R. SCHMID, *Scan. Electron. Microsc. II* (1986) 377.
6. P. J. MOELLER and J. W. HE, *Nucl. Instrum. Meth. Phys. Res.* **B17** (1986) 137.
7. E. GILLET, C. le GRESSUS and M. GILLET, *J. Chim. Phys.* **84** (1987) 167.
8. C. JARDIN, "Le Vide, Les Couches Minces", n° Special (1988) 95.
9. J. CAZAUX and C. le GRESSUS, *Scan. Microsc.* (1991) to be published.
10. J. VINE and P. A. EINSTEIN, *Proc. IEE* **111** (1964) 921.
11. K. LIANG, G. ORANGE and G. FANTOZZI, *J. Mater. Sci.* **25** (1990) 207.
12. C. JARDIN, P. DURUPT, D. ROBERT, P. MICHEL and C. le GRESSUS, *Mater. Sci. Engng* **B7** (1990) 119.
13. K. H. LEE and J. H. CRAWFORD Jr., *Phys. Rev.* **B15** (1977) 4065.
14. *Idem, ibid.* **B19** (1979) 3217.
15. B. G. DRAEGER and G. P. SUMMERS, *ibid.* **B19** (1979) 1172.
16. V. I. BARYSHNIKOV, E. F. MARTYNOVICH, T. A. KOLESNIKOVA and L. I. SHCHEPINA, *Sov. Phys. Solid State* **30** (1988) 868.
17. C. le GRESSUS and P. MAIRE, *J. Chim. Phys.* **84** (1987) 295.

Received 17 May
and accepted 26 June 1990